Robust Pupil Localization Algorithm Based on Circular Hough Transform for Extreme Pupil Occlusion

Muhammad Taufiq Setiawan, Sunu Wibirama*, Noor Akhmad Setiawan
Department of Electrical Engineering and Information Technology
Faculty of Engineering, Universitas Gadjah Mada
Yogyakarta 55281 Indonesia

***Abstract*—Pupil localization has been the core of eye tracking research. Accuracy of an eye tracking application relies on how center of the pupil is localized under various occlusions—such as eyelids and eyebrows. Previous works have preserved the accuracy of pupil localization when the eyelid covers the pupil up to 70% occlusion. However, the existing algorithm fails to maintain accuracy of pupil localization when the coverage of the occlusion is 70% or more. To deal with this problem, we propose a robust pupil localization algorithm based on circular Hough transform. The proposed algorithm was tested on 37 images taken from CASIA Iris dataset with various simulated eyelid occlusions. Our method achieved significant accuracy compared with previous state-of-the-art method—yielding 90.71% accuracy on 90% eyelid occlusion. The experimental results demonstrate that the proposed algorithm is promising to handle extreme eyelid occlusion in various eye tracking applications.**

***Index Terms*—Eye tracking, Pupil localization, Eyelid occlusion, Circular Hough transform**

I. INTRODUCTION

Eye tracking is an important research area with wide range of applications, such as human-computer interaction [1], computer-aided diagnosis for psychological [2], neurological, or ophthalmological disorders [3], virtual reality and 3D graphics [4–6], as well as an assistive system for disabled people [7, 8]. Accuracy of an eye tracking application depends heavily on how center of the pupil is estimated and localized (see Fig. 1). For instance, even one pixel loss on the estimated coordinates of the pupil may induce significant error of gaze direction vector, which in turn resulting a drift in the estimated point of gaze. In a computer-aided diagnosis system, errors in estimating pupil center affect accuracy of the estimated eye movements [9].

Pupil localization based on image processing techniques has been implemented using three main approaches: center of gravity [10, 11], ellipse fitting [12, 13], and curvature algorithm [14]. Center of gravity algorithm is based on estimating statistical moment of pupil contour. Statistical moment can be defined as a gross characteristic of the pupil contour by integrating or summing over all pixels of the contour. On the other hand, pupil localization based on ellipse fitting technique is performed by fitting an ellipse model to the detected pupil contour. Eventually, ellipse fitting works well when the distance between the ellipse points and the contour points is minimum.

*Corresponding author. Tel.:+62-274-552305. Address: Intelligent Systems Research Group, DTETI Bld., Jalan Grafika 2 Yogyakarta 55281 Indonesia. Email: muhammad.taufiq.s@mail.ugm.ac.id, {sunu, noorwewe}@ugm.ac.id

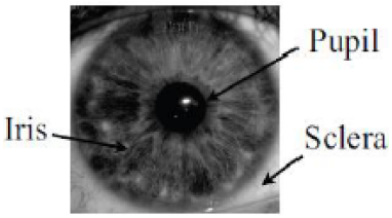

Fig. 1. Three components of human eye: pupil, iris, and sclera. Pupil localization aims to detect center of the pupil regardless of occlusion of eyelid or eyebrow.

Center of gravity and ellipse fitting are commonly used in real-time eye tracking as both algorithms require minimum computational resources. However, these methods are prone to error due to the irregularity of pupil shape, poor contrast, and unwanted corneal reflection resulting from light sources. To solve these drawbacks, a new approach of pupil localization based on curvature algorithm is later introduced by Krisnamoorthi and Annapoorani [14]. This algorithm yields high accuracy, but the method may cause false results due to curvature transition from the eyelid to the visible pupil.

In the previous study [15], Satriya et al. introduces an improved ellipse fitting algorithm by implementing adaptive image binarization based on cumulative histogram and Random Sample Consensus (RANSAC) for outliers removal. RANSAC is used during fitting an ellipse to the extracted pupil contour. They implement the algorithm in static images and videos of an eye tracking system. Their method improves accuracy of the conventional ellipse fitting algorithm up to 51% on 90% occlusion of eyelid. Unfortunately, the improved ellipse fitting algorithm does not preserve 80% accuracy of the estimated pupil coordinates when the pupil is covered 70% or more. In this case, the improved ellipse fitting algorithm is not appropriate for extreme pupil occlusion with 70% or more

978-1-5386-5813-0/18/$31.00 ©2018 IEEE

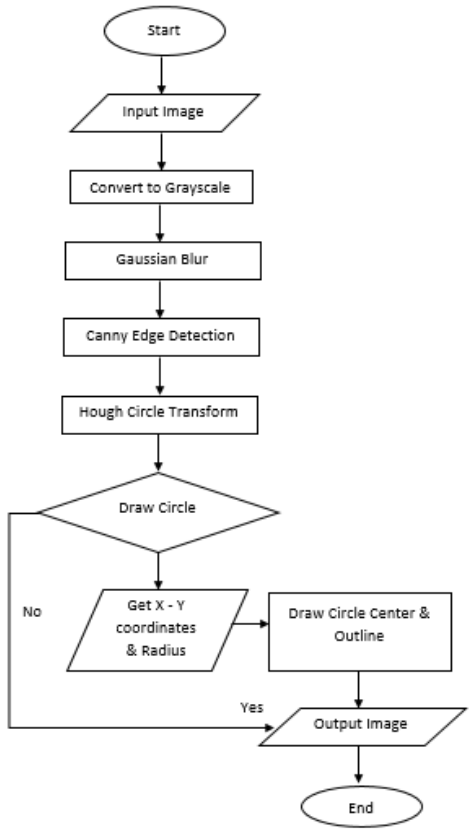

Fig. 2. Flowchart of proposed algorithm

eyelid coverage. Furthermore, RANSAC is a non-deterministic algorithm that leads to unstable result in every tracked video frame.

To overcome this research gap, we propose a robust pupil localization algorithm based on circular Hough transform. The mapping between the image and the parameter space was performed by Hough transform [17, 18]. In the parameter space, pixels of the edges are mapped into the cells. The information that is related to the parameters of the pixels is stored in an accumulator. At the end of the process, the local maximum of the accumulator finds the parameters that corresponds to the specified shape. We compared our method with an improved ellipse fitting algorithm [15]. Comparative analysis of the accuracy shows that our algorithm is superior in handling extreme occlusion compared with the previous method [15].

II. MATERIALS AND METHODS

The proposed method consists of two main steps: acquisition of grayscale image and implementation of hough circle transform. The proposed algorithm is shown in Fig. 2.

A. Gaussian Blur

We used similar dataset as used in previous works [15, 16]. In the grayscale image, intensity levels are divided into black, white, and some levels between black and white. To eliminate noises in the grayscale image, we use Gaussian blur as a filter. Gaussian filtering is done by convolving each point in the input array with a Gaussian kernel and then summing them to produce the output array. In 2D Euclidean space, the equation of a Gaussian filter is represented as

$$G(i,j) = \frac{1}{2\pi\sigma^2} exp\left(-\frac{(i-(k+1))^2 + (j-(k+1))^2}{2\sigma^2}\right) \quad (1)$$

where i is the distance from the origin in the horizontal axis, j is the distance from the origin in the vertical axis, and σ is the standard deviation of the gaussian distribution. The kernel size $(ksize)$ is $1 \leq i, j \leq (2k+1)$. In this research, we used kernel size of 7 x 7 , 9 x 9 and combination between 9 x 7 or 7 x 9

B. Canny Edge Detection

Canny edge detector is used to detect the edge of the pupil. The edge detector works in a single entity with the Hough transform. The first parameter value that we choose for upper threshold in the internal Canny edge detector is 100, while the second parameter values to be the threshold for center detection are 17 or 12 or 10. Those values are chosen based on empirical experiment. G and Θ are defined as edge gradient and edge direction, respectively. Canny edge detection can be formulated by Eq.(2) and (3):

$$G = \sqrt{{G_x}^2 + {G_y}^2} \quad (2)$$

$$\Theta = atan2(G_x, G_y) \quad (3)$$

G_x and G_y represent edge in horizontal and vertical direction, respectively.

C. Circular Hough Transformation

In 1962, Hough transformation was introduced and mentioned as a robust algorithm to detect features of certain shapes such as lines or circles in digital images [19]. Hough circle transformation can be used to infer radius of circular shape. In our case, human's pupil can be identified as circular shape. Unlike edge detectors, Hough transform is more tolerant to gaps in features that describe the borders and more robust to noise.

The general principle of Hough transform is represented by *N*-dimensional projections of the image space to the parameter space with dimensions *M*, associated with a particular mathematical model. The formula of the Hough circle is shown in the Eq.(4):

$$(x-a)^2 - (y-b)^2 - r^2 = 0 \quad (4)$$

Based on Eq.(4), there are only three parameters in parameters space: two parameters used for the center of the circle (a, b) and one parameter used for the radius of the circle (r). For more complex geometry, the dimension of Hough space will increase due to increment of the number of variables.

Based on the Hough transform for circles, each pixel in the image space fits to a circle in the hough space and otherwise (see Fig. 3). All points of the circle C in the image are

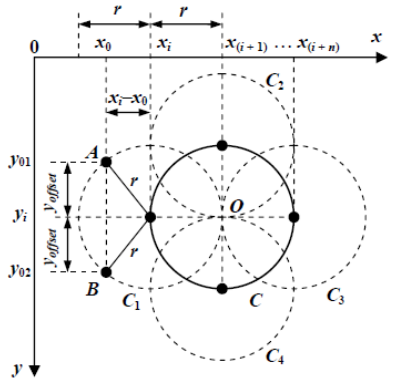

Fig. 3. The Hough transform principle.

transformed in several circles (C_1, C_2, C_3, C_4) with the same radius *r*, where their intersection, O, is the center of the detected circle. The coordinates on the *Y* axis of the two symmetrical points A and B (with the same coordinates x_0 on the *X* axis,) on the Hough circle C_1 of Fig. 3 are given by the following equations:

$$\begin{cases} y_{01} = y_1 - y_{offset} \\ y_{02} = y_2 + y_{offset} \end{cases} \tag{5}$$

where y_{01} and y_{02} are row coordinates of the detected circles while y_1 and y_2 are index in Y axis of edge pixels.
The offset of the *Y* axis is shown by equation

$$y_{offset} = \sqrt{r^2 - (x_i - x_0)^2} \tag{6}$$

where y_{offset} is cartesian offsets of row coordinates, r is the radius of the circle and x_i and x_0 is column coordinates of detected circles. The Hough accumulator is the result of the Hough transform. The accumulator stores its values on a table that has similar size as the size of the original image. The value of the accumulator will be updated by using Hough transform for each circle. The points on the Hough circles contain address of accumulator. The addresses ($C1$, $C2$, $C3$, $C4$) are increased by one unit. The center O of the detected circle C is the maximum value of the accumulator.

The Hough transform for circle detection is useful to solve cases with two conditions [18]:

- The condition of known radius: it means a pair of coordinates (x_i, y_i) represent the centre of Hough circles. The Hough space with this condition is called bidimensional.
- The condition of unknown radius: this condition has three parameters (x_i, y_i, r_i). They represent the coordinates of the Hough circles and its radius. Therefore, the Hough space is called tridimensional.

D. Accumulator and Voting

The number of "circles" in the parameter space passing through the grid cell are elements in the accumulator matrix or referred to as the "voting number". Mainly, every element in the matrix is zero. "Voting" is performed to formulate the circle in the parameter space. Local maxima in the accumulator matrix can be found after voting. Additionally, the positions correspond to the circle centers in the original space. The algorithm of Hough circle transform and the voting mechanism are shown in Algorithm 1 and Algorithm 2, respectively.

Algorithm 1 Hough circle transform algorithm

```
procedure HOUGH CIRCLE
    for each node each A[a, b, r] = 0 do
        Process of Gaussian Blurring
        Grayscale image converting
        Make Canny operator
        Vote in accumulator.
    end for
end procedure
```

Algorithm 2 Hough circle transform voting

```
for each pixel(x, y) do
    for each radius r = 10 to r = 60 do
        for each θ t = 0 to 360 do
            a = x  r * cos(t * φ / 180)
            b = y  r * sin(t * φ / 180)
            A[a,b,r] +=1
        end for
    end for
end for
```

E. Accuracy Measurement and Comparison

We performed exactly similar procedures as conducted by Satriya et al. [15] to verify our algorithm. We evaluated the proposed algorithm on static eye images from *Chinese Academy of Sciences Institute of Automation* (CASIA) dataset [16]. The dataset was collected from 1,000 participants with 10 times recording for each participant. All 37 images used in the previous study were used in this study. We directly compared accuracy of the proposed method with an improved ellipse fitting method [15]. The formulas to measure accuracy are shown below:

$$err = \sqrt{(x - x')^2 + (y - y')^2} \tag{7}$$

$$acc = \left(1 - \frac{err}{radius}\right) * 100\% \tag{8}$$

As shown in Eq.(7), err is defined as an absolute error in pixel. Hough circle center in *X* axis is defined by x, while y is defined as a Hough circle center in *Y* axis. Reference of Hough circle is center in *X* axis is defined by x' and reference of Hough circle center reference in *Y* axis is defined by y'. Accuracy is represented by acc. The radius of the Hough circle is represented by $radius$. The results of our method will compared by using Z-test and the significance value of 5% as proposed by Satriya et al. [15].

TABLE I
COMPARATIVE ANALYSIS OF PUPIL TRACKING ALGORITHMS WITH RESULTS OF Z-TEST

Occlusion (%)	The proposed method (in pixel)		Improved ellipse fitting [15] (in pixel)		Z-score
	Mean	S.D.	Mean	S.D.	
10	98.88	2.02	98.32	1.45	3.32 (**)
20	98.32	2.36	96.53	4.08	2.96 (**)
30	98.04	2.49	94.05	7.65	2.28 (**)
40	98.02	2.45	89.29	12.57	1.97 (**)
50	97.93	2.66	83.65	17.32	1.72
60	96.54	3.95	79.04	20.95	1.42
70	96.02	3.63	75.79	25.16	1.16
80	95.47	3.62	51.42	30.61	1.71
90	90.71	9.48	19.28	18.49	6.12 (**)

(**) : significant result

Figure 4 shows eye images that were modified with various eyelid occlusion ranging from 10% to 90% coverage. The modification aimed to systematically simulate real eyelid occlusion while observing robustness of the proposed algorithm.

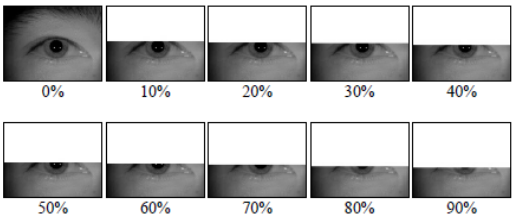

Fig. 4. Modified pupil with variation occlusion

III. RESULTS AND DISCUSSION

Figure 6 and Table 1 show comparative analysis of pupil localization accuracy between our proposed method and improved ellipse fitting method [15]. We used two-tailed Z-test with critical values of 1.96 and -1.96. That is, the difference between both algorithms is significant if the Z-value is less than -1.96 or more than 1.96. In this case, Z-test shows that the results differ significantly during 10% and 90% occlusion. We achieved

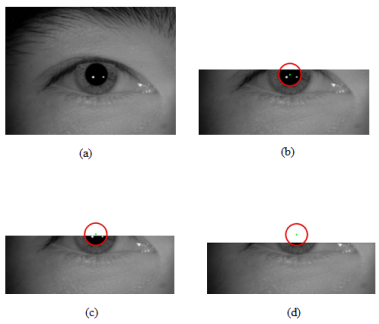

Fig. 5. (a) Pupil without eyelid occlusion; comparative analysis of pupil localization during various occlusion: (b)30%; (c)60%; (d)90%.

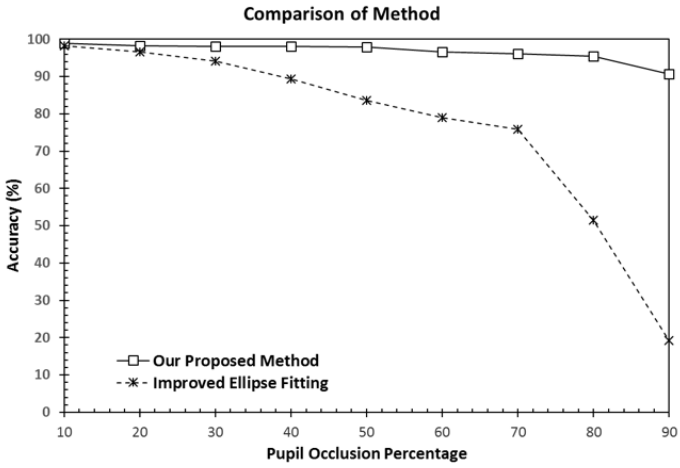

Fig. 6. Comparison of accuracy (in %) between our purposed method and improved ellipse fitting proposed by Satriya et al. [15]

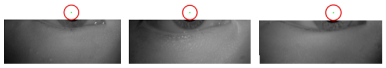

Fig. 7. Sample of several pupil localization errors during extreme eyelid occlusion (90% coverage of pupil).

significantly higher accuracy during 90% eyelid occlusion (M = 90.71%) compared with improved ellipse fitting method (M = 19.28%). Although overall accuracy of our proposed method is still above 80%, in some cases Hough circle transform failed to correctly identify the pupil position, resulting in errors of pupil center coordinates as shown in Fig. 7.

Figure 8 shows graphical plot of standard deviation between the proposed algorithm and the improved ellipse fitting algorithm. The proposed algorithm yielded more stable results of pupil localization compared with previous work. In this study, we did not include any non-deterministic algorithm—such as RANSAC—as used in the previous work [15]. RANSAC generally poses unstable results, as result of one iterative computation will be different from the other iterations. Our choice of im-

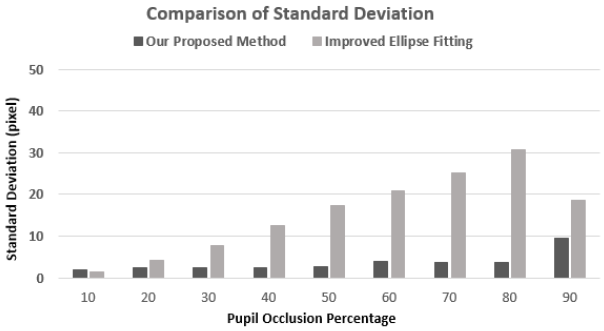

Fig. 8. Comparative analysis of standard deviation between the proposed method and improved ellipse fitting [15] (in pixel).

TABLE II
COMPARISON OF COMPUTATIONAL TIME (IN MS).

Algorithm	**The proposed method**	**Improved ellipse fitting [15]**
Computational time	0.30 ms	3.09 ms

plementing Hough transform also reduced computational time needed to find the center of pupil (see Table 2). The proposed algorithm was 11 times faster than previous work. However, the proposed method worked under several constraints—Hough transform parameter was adjusted empirically during the experiment (i.e., ranging from 25–65) while the proposed algorithm has not been tested yet in real-time video streaming. In future, we intend to improve our algorithm by incorporating adaptive mechanism for Hough transform parameters.

IV. CONCLUSIONS

Pupil localization has been an important part in improving accuracy of various eye tracking applications. Previous work of pupil localization based on improved ellipse fitting algorithm has not been able to preserve 80% accuracy when the pupil is covered 70% or more. To solve this gap, we propose a new approach by incorporating Hough circle transform for pupil localization. The proposed algorithm was tested on static image dataset with various simulated eyelid occlusions, ranging from 10% to 90% coverage. Experimental results show that the proposed algorithm was superior than the improved ellipse fitting algorithm as it could preserve more than 80% accuracy during 70% or more eyelid coverage. During 90% pupil occlusion, the proposed algorithm achieved significantly higher accuracy (M = 90.71%) with 11 times faster computational time compared with the improved ellipse fitting algorithm (M = 19.28%). These results imply that the proposed algorithm is promising to handle extreme eyelid occlusion in various eye tracking applications.

REFERENCES

[1] S. Wibirama, H. A. Nugroho, K. Hamamoto, "Evaluating 3D gaze tracking in virtual space: A computer graphics approach", *Entertainment Computing*, Vol. 21, pp. 11-17, 2017.

[4] S. Wibirama, K. Hamamoto, "Investigation of visually induced motion sickness in dynamic 3D contents based on subjective judgment, heart rate variability, and depth gaze behavior," in *2014 36th Annual International Conference of the IEEE Engineering in Medicine and Biology Society (EMBC 2014)*, Chicago, US, 2014, pp. 4803-4806.

[2] S. Wibirama, H. A. Nugroho, "Towards understanding addiction factors of mobile devices: an eye tracking study on effect of screen size," in *2017 39th Annual International Conference of The IEEE Engineering in Medicine and Biology Society*, Jeju Island, South Korea, 2017, pp.2454-2457.

[3] S. Wibirama, S. Tungjitkusolmun, C. Pintavirooj, "Dual-camera acquisition for accurate measurement of three-dimensional eye movements," *IEEJ Transactions on Electrical and Electronics Engineering*, Vol.8, No. 3, pp. 238-246, 2013.

[5] M. Bahit, S. Wibirama, H. A. Nugroho, T. Wijayanto, M. N.Winadi, "Investigation of visual attention in day-night driving simulator during cybersickness occurrence", in *2016 8th International Conference on Information Technology and Electrical Engineering (ICITEE 2016)*, Yogyakarta, Indonesia, 2016, pp. 213-216.

[6] S. Wibirama, H. A. Nugroho, K. Hamamoto, "Depth gaze and ECG based frequency dynamics during motion sickness in stereoscopic 3D movie," *Entertainment Computing*, Vol. 28, pp. 117-127, 2018.

[7] V. Pasian, F. Corno, I. Signorile, L. Farinetti, "The Impact of Gaze Controlled Technology on Quality of Life," in *Gaze Interaction and Applications of Eye Tracking: Advances in Assistive Technologies*, IGI Global: Hershey PA, 2012, pp. 48-54.

[8] M. Borgestig, J. Sandqvist, R. Parsons, T. Falkmer, H. Hemmingsson, "Eye gaze performance for children with severe physical impairments using gaze-based assistive technologyA longitudinal study," *Assistive technology*, Vol.28, No.2, 2016, pp.93-102.

[9] T. Tanaka, S. Tominaga, "Analysis of rotational vertigo using video and image processing," in *2011 4th International Conference of Biomedical Engineering and Informatics (BMEI 2011)*, Shanghai, China, 2011, pp. 122-127.

[10] T. Yagi, "Nystagmus as a sign of labyrinthine disorders – three-dimensional analysis of nystagmus," *Clinical and Experimental Otorhinolaryngology*, Vol.1, pp.63-74, 2008.

[11] H.G. MacDougall, K.P. Weber, L.A. McGarvie, G.M. Halmagyi, I.S. Curthoys, "The video head impulse test Diagnostic accuracy in peripheral vestibulopathy," *Neurology*, Vol. 73, No. 14, pp.1134-1141, 2009.

[12] A.B. Roig, M. Morales, J. Espinosa, J. Perez, D. Mas, C. Illueca, "Pupil detection and tracking for analysis of fixational eye micromovements," *Optik-International Journal for Light and Electron Optics*, Vol. 123, No. 1, pp. 11-15, 2012.

[13] W. Swart, C. Scheffer, K. Schreve, "A Video-oculography based telemedicine system for automated nystagmus identification," *Journal of Medical Devices*, Vol. 7, No. 3, pp.031002, 2013.

[14] R. Krishnamoorthi, G. Annapoorani, "A simple boundary extraction technique for irregular pupil localization with orthogonal polynomials," *Computer Vision and Image Understanding*, Vol. 116, No. 2, pp. 262-273, 2012.

[15] T. Satriya, S. Wibirama, I. Ardiyanto, "Robust Pupil Tracking Algorithm based on Ellipse Fitting," in *2016 IEEE International Symposium on Electronics and Smart Devices*, Bandung, Indonesia, 2016, pp. 253-257.

[16] CASIA Iris Database, National Laboratory of Pattern Recognition (NLPR), http://biometrics.idealtest.org/dbDetailForUser.do?id=4 (Accessed: October 23*th*, 2017).

[17] Y. Xie, Q. Ji, "Effective line detection with error propagation," *Proceedings of 2001 IEEE International Conference on Image Processing*, Vol.1, 2001, pp. 181-184.

[18] N. Cherabit, F.Z. Chelali, A. Djeradi, "Circular Hough Transform for Iris localization," *Science and Technology*, Vol. 2, No.5 pp.114-121, 2012.

[19] R. Duda, P. Hart, "Use of the Hough transformation to detect lines and curves in pictures," *Communication of the ACM*, Vol. 15, No. 1, pp.11-15, 1972.